RSC Advances

ROYAL SOCIETY OF CHEMISTRY

www.rsc.org/advances

Cite this: DOI: 10.1039/c0xx00000x

www.rsc.org/xxxxxx

ARTICLE TYPE

Molecular interactions of ethylcellulose with sucrose particles

Terri A. Stortz[a], Dref C. De Moura[b], Thamara Laredo[c] and Alejandro G. Marangoni[a]*

Received (in XXX, XXX) Xth XXXXXXXXX 20XX, Accepted Xth XXXXXXXXX 20XX
DOI: 10.1039/b000000x

Recent work has shown that sucrose crystals have the ability to interact with ethylcellulose (EC) and form a network within food materials that provides mechanical strength and affects stability. We recently reported on the ability of EC to impart heat resistance in chocolate.[1] Evidence suggests that the sucrose present in the chocolate plays a major role in the heat resistance. Here we show that EC is able to hydrogen bond with sucrose which allows for the creation of an oil-trapping network. Atomic scale molecular dynamics simulations and FTIR spectroscopy both showed the ability of EC to hydrogen bond with sucrose. Texture analysis and scanning electron microscopy showed the ability of EC and sucrose to form a network within an oil medium which resisted deformation. It was also shown that lecithin at the surface of the sucrose impedes EC-sucrose interactions. These results have lead to an understanding of the mechanism of heat resistance in EC solvent substitution chocolate and will be useful in developing new food products containing EC as a functional ingredient that enhances the sugar network. Furthermore, there is evidence that a strong, heat resistant network can be created for various particles other than sucrose including glucose, starch, and even diamond dust.

Introduction

It has previously been shown that addition of ethylcellulose (EC) to conventional chocolate using the "solvent substitution" method results in the production of a chocolate with substantial heat resistance.[1] A heat resistant chocolate is one that can resist melting or deformation at temperatures above 34°C, the normal melting temperature of chocolate.[2] Many methods have been developed to produce heat resistant chocolate,[3] but the addition of EC to induce heat resistance in chocolate represents a novel technique.

Although an explicit explanation for the mechanism of heat resistance in chocolate cannot be found in the literature of patents, several important observations have been made. In general, the creation of a sugar network in the chocolate using a variety of techniques is always hinted at.[3] The secondary sugar network would allow the chocolate to hold its shape when the primary fat crystal network has melted. In particular, three ways to accomplish the formation of such network have been patented in the past: Either by wetting the surface of the sucrose crystals with small amounts of water so that it becomes "sticky" and aggregates with other solid particles in the chocolate[4]; by using large amounts of water to completely dissolve the sucrose, and then evaporating the water in order to leave behind a recrystallized sucrose network[5]; or by preventing the sucrose crystals in the chocolate from being fully coated with fat, leaving some surfaces of the crystals available to stick to one another and form a network.[6]

In our previous paper, we showed that the EC solvent substitution (SS) method, produces a chocolate that has a hardness of 18 N at 40°C.[1] The work here presented explores the hypothesis that EC and sucrose interact to create a network within the chocolate that leads to the observed heat resistance.

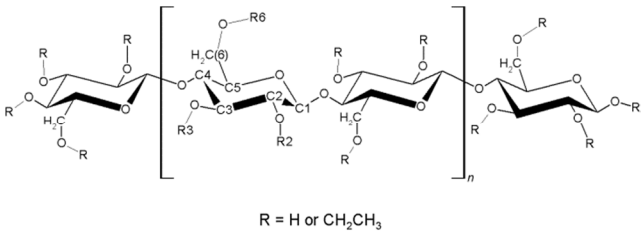

Fig. 1 Structure of ethylcellulose with carbon and R-group numbering system

EC is a linear polymer of β-1,4 linked D-glucose units with some of the hydroxyl groups substituted with ethoxyl groups (Figure 1). There are three hydroxyl groups on each monomer (excluding terminal monomers) that are available for ethoxylation. The degree of substitution is controlled during manufacture. Commercially produced EC that is soluble in organic solvents has a degree of substitution of 2.3-2.6 (out of a maximum of three).[7] The EC polymers used in this study were specified as having an ethoxyl content of 48-49.5% which corresponds to a degree of substitution of 2.47-2.58. Previous studies[8-10] have shown that the distribution of ethoxyl groups on the monomers is not random. The group showing lowest reactivity is R3. This is thought to be a consequence of intramolecular bonding between the hydrogen of the hydroxyl group at R3 and the ring-oxygen atom in adjacent monomers.[8] Interestingly, it has been found that the relative reaction rate of ethoxylation at R3 increases when R2 is ethoxylated which is

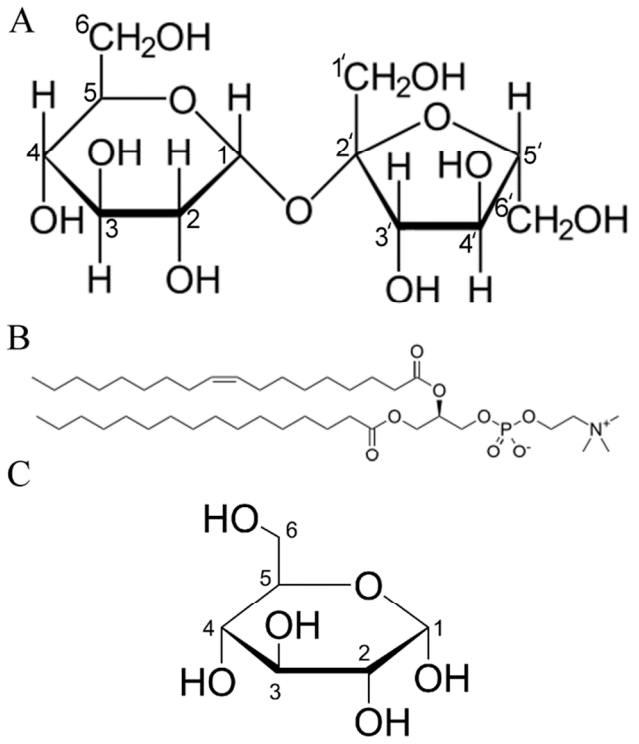

Fig 2. Structure of (A) sucrose with carbon numbering system, (B) phosphatidylcholine, and (C) glucose

thought to be due to the disruption of the intramolecular hydrogen bond.[9] On the other hand, the hydroxyl group at R6 has been found to be the most reactive.[9, 10] With three hydroxyl groups available for ethoxylation there are eight possible monomers in an EC polymer. The concentrations of each type of monomer were not available for the EC polymers used. Therefore, these values were found in the literature and used as close approximations for what would be present experimentally.

It is not obvious from the literature whether interactions can exist between EC and sucrose. Ibrahim *et al*.[11] coated sucrose crystals with EC by first dissolving the EC in absolute ethanol (EtOH) and thereafter evaporating the EtOH. The EC coating was used to reduce the solubility of sucrose in an aqueous system for the purpose of understanding the effect of excipient solubility on the dissolution of a drug prone to agglomeration. Scanning electron microscopy photomicrographs showed that the EC covered the sucrose, with dissolution only taking place at holes in the coating where the aqueous phase was able to penetrate. Sucrose was also mentioned as a low molecular weight additive which can be used to increase the permeability of an EC coating for controlled-release of pharmaceuticals.[12] Considering the structure of EC and sucrose (Figure 2A) it is thought that hydrogen bonding may occur between polar groups on EC, such as unsubstituted hydroxyl groups on the EC chain, and free hydroxyl groups on the sucrose crystal.

In conventional chocolate, it is also important to consider the possibility of an interaction between EC and the lecithin phospholipids present at the surface of sucrose. A specific interaction between soybean phospholipids and EC has not been shown in the literature. However, interactions between EC and

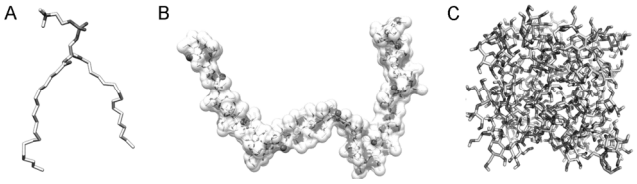

Fig. 3 Stick and space filling representations of: (A) POPC; (B) EC30 with hydroxyl groups indicated by dark spheres; (C) sucrose crystal. Images are not on the same scale

dialkyl phthalates[13], propylene glycol dicaprylate/dicaprate[14], and nifedipine[15] have been found. All of these molecules have similar structure to phosphatidylcholine (PC) (Figure 2B), an abundant phospholipid in soybean lecithin. It is thought that since the hydroxyl groups on EC are slightly polarized, they can hydrogen bond to the slightly polarized carbonyl groups at the ester linkage in PC. In contrast, no interactions were found between the carbonyl groups on triglycerides and EC.[16] If an interaction between EC and PC exists then perhaps the PC can act as a bridge between EC and sucrose during network formation. We present in this paper evidence of molecular interactions between the different components present, which are responsible for the heat resistance displayed by EC containing chocolate.

Table 1 Proportions of monomers in the EC30 molecule

Monomer*	Literature[17] (%)	Experimental (%)	Difference (%)
-	0.42	0	0.42
6	0.63	0	0.63
3	0.21	0	0.21
2	0.42	0	0.42
2,3	2.71	3.33	0.62
2,6	16.48	16.67	0.19
3,6	4.17	3.33	0.84
2,3,6	74.97	76.67	1.69
			Total = 3.34

*Numbers represent positions of ethoxy substitution(s) (see Figure 2A for numbering scheme)

Materials and methods

Atomic scale molecular dynamics (MD) simulations

Atomic scale molecular dynamics simulations were performed to explore the hypothesis that EC and sucrose can hydrogen bond to one another. The interactions between a representative EC molecule and a PC, specifically 1-palmitoyl-2-oleoyl-sn-glycero-3-phosphocholine (POPC) (Figure 3A), and POPC and sucrose were also explored. The polymer was only 30 monomer units in length due to computing limitations. The proportions of each of the eight possible EC monomers were chosen based on the work by D'Ambra et al.[17] and are shown in Table 1. D'Ambra et al. used a commercially available EC with a degree of substitution of 2.66. This degree of substitution was slightly higher than the degree of substitution for the EC polymers used experimentally which was 2.47-2.58. Nevertheless, the proportions found by D'Ambra et al. were thought to give a relatively good estimate of the monomer proportions present in the EC used. This molecule will be hereafter referred to as "EC30". The sequence of monomers in EC30 (Figure 3B) was chosen deliberately to have three fully ethoxylated monomers between each doubly ethoxylated monomer since the presence of the former is much greater than the latter. A representative sucrose crystal (Figure

3C) was built by adding 41 sucrose molecules to a 3 nm2 unit cell and running an unrestrained simulation for 5 ns to allow the sucrose molecules to orient themselves in a crystal structure,

Table 2 Proportions of monomers in the co-block and ordered EC62 polymers

Monomer	Literature[7] (%)	Experimental (%)	Difference (%)
-	0.10	0.00	0.10
6	1.59	1.61	0.02
3	0.20	0.00	0.20
2	1.59	1.61	0.02
2,3	3.28	3.23	0.06
2,6	22.59	22.58	0.01
3,6	4.78	4.84	0.06
2,3,6	65.87	66.13	0.26
			Total = 0.73

maximizing hydrogen bonds between their hydroxyl groups. Simulations were performed using GROMACS 4.5.5 software suite.[18-21] which uses classical mechanics to determine the trajectories of atoms over a specified time-course based on a coordinate file of the molecule. The reader can refer to van der Spoel *et al.* (2002)[22] for more information. Sucrose and EC were built using the 53A6[23] subset of the GROMOS force field, with parameters adapted from the 45A4[24] subset for pure carbohydrate systems and subsequent re-optimized parameters from the 56Acarbo[25] force field. Parameters for the ethoxy groups were adapted from parameters developed for ethoxyethane from the Automated Topology Builder web server.[26] POPC parameters were taken directly from work previously done by Tieleman *et. al*.,[27] with parameters for triolein adapted from the acyl chains of POPC. Periodic boundary conditions were used for all simulations. Short-range electrostatics were cut off at 0.9 Å and long-range electrostatic interactions were calculated using the particle-mesh Ewald method. To calculate van der Waals interactions, a twin-range scheme was employed (0.9/1.4 Å). A 2 fs integration time step was used with neighbour searching performed every 5 ps. The Berendsen weak coupling[28] method was used to couple temperature and pressure using the velocity rescale thermostat[29] ($\tau t = 0.1$) and Parrinello-Rahman[30] barostat ($\tau p = 0.5$) respectively at 307.15 K and 1 bar. Avogadro 1.0.3[31] was used to build the initial structures for both the EC and triolein molecules. Hydrogen bonding was analysed using a program which identifies these bonds based on two geometrical criteria:

$$r \le r_{HB} = 0.35\ nm$$
$$\alpha \le \alpha_{HB} = 30°$$

where r is distance between donor and acceptor and α is the angle between hydrogen donor and acceptor.[22] These values are based on observations of hydrogen bonding found in water and are widely used in analysis of molecular simulations.[22]

The system was reevaluated and several changes were made prior to moving forward with subsequent simulations. Two new EC molecules of 62 monomers length were built with proportions of monomers based on the work by Rosell[7] and are given in Table 2. Rosell analyzed EC with a degree of substitution of 2.64, similar to D'Ambra *et al*. and still higher than the DS of the EC used experimentally. However, Rosell found slightly different proportions of monomers than D'Ambra. The differences observed were likely due to the different methods used which have been described in detail elsewhere[7, 17]. The proportions determined by Rosell and use of a longer molecule permitted the inclusion of a greater number of hydroxyl groups within the EC molecule allowing for a greater number of possible hydrogen bonds to be observed. The distribution of each of the monomers in an EC polymer is unknown therefore two distinctly different distributions were chosen to be studied. The first new EC molecule had two fully ethoxylated monomers between each of the hydroxylated monomers and will be henceforth denoted as "ordered" polymer. The second polymer had blocks of five hydroxylated monomers between ten fully ethoxylated monomers and will be denoted as "co-block" polymer. The large blocks of hydroxylated monomers may mimic a crystalline region along the EC that was unable to be ethoxylated during manufacture.

Four new systems were studied utilizing the ordered and co-block EC, POPC, the sucrose crystal, and triolein as a representative triglyceride. The first system included the EC molecule solvated in triolein; the second system had sucrose crystals placed next to the EC molecule and this was solvated in triolein; the third system had the sucrose crystals coated in POPC next to EC molecules and this was solvated in triolein; the fourth system had EC solvated in triolein with sucrose crystals randomly placed within the simulation space (at a further distance from EC than system two). The simulations were performed and analyzed using the same settings as described in Part 1 except that the temperature was chosen as 40°C to mimic the temperature used when performing heat resistance tests.

Hardness tests of model systems

Model chocolate systems based on the ingredients in solvent substitution (SS) chocolate were prepared using the following ingredients: granulated sucrose (Red Path, Toronto ON), EC 10 cP (Dow Chemicals, Midland, MI), palm kernel oil (PKO) (Nealander's International Inc., Mississauga, ON), soybean lecithin (Grain Process Enterprises Ltd. Scarborough, ON), glycerol monooleate (GMO) (Hallstar, Chicago IL), sorbitan monooleate (SMO) (Sigma Aldrich, St. Louis, MO), Alphadim 90 SBK glycerol monostearate (GMS) (Caravan Ingredients, Lenexa, KS), Grinsted sorbitan monostearate (SMS) (Danisco, Scarborough, ON), and absolute ethanol (EtOH) (Commercial Alcohols, Brampton, ON).

Two methods were used for preparation of these samples: the solvent substitution (SS) method; and the heat method. Granulated sucrose was chopped in a blender prior to use, to reduce the particle size. For the SS method the PKO was melted and the sucrose, when used, was added and thoroughly mixed. If sucrose was not added then the PKO was left at room temperature to begin crystallisation. Once crystallisation began the PKO was stirred occasionally until it was partially crystalline but still flowable. EC 10 cP from a 20% EC in EtOH mix was then added to the PKO or PKO and sucrose mixture and stirred for 1 min using an overhead stirrer at 200 rpm with a paddle impeller. The sample was then moulded, cooled at 5°C for 20-30 min, and demoulded by rapping the mould on a counter. The mould produced samples in tablet form with dimensions of 3.60 cm (l) x 1.90 cm (w) x 0.68 cm (d). The samples were left overnight and then placed in an incubator at 30°C for sufficient time to evaporate the EtOH.

Heat method samples were prepared by dissolving the EC in the PKO, with surfactant if used, in a beaker with heating (up to around 140°C) and stirring. It was required to heat the sample to

140°C, the glass transition temperature of EC, to fully dissolve the EC. For samples containing sucrose the EC and PKO was poured into the sucrose sample once cooled slightly (around 110°C). The sucrose was kept in a stainless steel 250 mL beaker that was held at 60°C using a dry bath with a custom fitted steel sample holder. This would ensure the temperature of the sample remained elevated during stirring and thereby minimizing the chances that the EC would set prior to the end of mixing. The sample was stirred for 1 min at 200 rpm using an overhead stirrer with a paddle impeller. The samples were then moulded, cooled, and demoulded as in the SS procedure.

Some heat method samples were also prepared with lecithin. The amount of lecithin added was calculated based on maintaining a ratio of lecithin to solids similar to what would be found in a chocolate made with the typical amount of 0.3% lecithin and 70% solids-non-fat. During preparation of these samples the lecithin was added to the molten EC in PKO gel once slightly cooled, just prior to mixing with the sucrose. The samples were then moulded, cooled, and demoulded as above.

Samples with sucrose were formulated to contain a final concentration of 2.17% EC. Sucrose-free controls were formulated based on the assumption that all of the EC present would be in the fat phase and not interacting with the sucrose. Therefore, these controls contained the same ratio of EC:PKO as the equivalent sample with sucrose.

All samples were tested for heat resistance using the method developed by Stortz and Marangoni.[1] A texture analyser (Stable Micro Systems Ltd., Surrey, UK) was used to perform a set displacement in compression test on a sample that had been incubated at 40°C for 2 h. The cylindrical probe with 1.80 cm diameter was lowered into the sample 4 mm and the force in N at 2 mm displacement was recorded. This force was then divided by the area of the probe in m^2 to give a value for the hardness in Pa. The data was then added to a log-log plot of hardness versus volume fraction (Φ) of solids. The Φ was calculated from the mass fraction of sucrose in the system and using the density to convert to a volume fraction. For the case of the sample with EC and no sucrose the Φ was calculated from the mass fraction of EC and converted using the density of EC. Linear regression was performed using GraphPad Prism 5.0 software.

Fourier transform infrared spectroscopy (FTIR)

FTIR spectroscopy was used to observe if chemical bonding occurs between EC and sucrose. Two sample preparation and analytical techniques were used. The first method followed a similar procedure to the SS method discussed previously. A solution of 20% EC 10 cP dissolved in absolute EtOH was prepared. Granulated sucrose was chopped in a blender and then the particle size was further reduced by grinding in a mortar and pestle. The EC was then mixed at various proportions with the sucrose. The mixture was occasionally mixed as the EtOH evaporated and spread to avoid producing clumps with EtOH filled centers. Once seemingly dried the mixture was then placed in an oven at 80°C for 1 h to evaporate any residual EtOH. The sample, which was quite chunky at this point, was then ground to a fine powder using a mortar and pestle. The sample was again incubated at 80°C for 1 h to evaporate any remaining solvent. After heating, the sample was placed in a dessicator to cool. Finally, the sample was capped and stored in the dessicator. Samples were prepared to produce mixes of 16, 33 or 50% EC on sucrose once dried.

Appropriate controls were also prepared. Control samples were prepared using the same procedures but did not contain EC. For example, the control for the 16% EC from EtOH sample was made by mixing sucrose with the same amount of EtOH as was present in the EC in EtOH sample. The EtOH was then evaporated, and the sample heated, ground, and heated again. Other controls included EC 10 cP powder and sucrose with no treatment.

A Thermo Fisher Scientific Nicolet 6700 FTIR spectrometer (Waltham, MA) with deuterated triglycine sulfate (DTGS) detector was used for analysis of the samples. Transmission mode was used for these powder-type samples. The spectra were collected as KBr pellets at 64 scans and had a resolution of 2 wavenumbers. Each sample was analyzed in triplicate.

The second method of sample preparation mimicked the heat method. EC 10 cP was dissolved in canola oil by heating to 140°C with stirring. Once fully dissolved the solution was mixed briefly by hand with finely ground sucrose. The sample was then cooled and stored in a dessicator. Samples were prepared with either 2 or 5% EC. Control samples contained heated oil and sucrose without any EC.

The heat method samples were analyzed using the same spectrometer and the attenuated total reflectance (ATR) sampling technique. The samples were spread onto a zinc selenide (ZnSe) crystal sample holder. The spectra were collected from 64 scans with a resolution of 2 cm^{-1}. Each sample was analyzed in triplicate.

Samples were also prepared with the addition of lecithin phospholipids. A crude extract of soybean phospholipids containing 14-23% phosphatidylcholine (PC) was obtained from Sigma-Aldrich (Saint Louis, MO). The PC was dissolved in chloroform to produce a 1% solution which allowed for the PC to be distributed onto the surface of the sucrose. The amount of PC added was representative of what is present in a typical chocolate and was calculated as follows: it was assumed that chocolate contains 50% sucrose and up to 0.5% lecithin[32] of which approximately 56% is phospholipids.[33] This gives an approximate phospholipid content of 0.28%. Considering a system of only the sucrose and phospholipids and ignoring the other components of the chocolate, the sucrose should be mixed with 0.6% phospholipids by weight. The PC in chloroform was added to finely ground sucrose and mixed using an overhead mixer. The chloroform was evaporated and a fine powder of PC coated sucrose was produced. This coated sucrose was then used to produce heat method samples and controls using the same procedures as outlined above. A control was also prepared with sucrose treated with chloroform but no PC.

Spectra were analyzed using Thermo Scientific OMNIC Spectra Software (Thermo Electron Scientific Instruments Corporation, Madison WI). Minimal processing techniques were used on the spectra to preserve the experimentally observed results. All spectra were first ratioed to their respective background spectra. For pellet type samples the background was a pellet of KBr with no sample present. For ATR samples the background was the ZnSe crystal with no sample present. Peak positions were then identified for samples and their respective

EC-free controls with particular focus on peaks for sucrose that have been identified in the literature.[34] The peak position (PP) for the sample was then subtracted from the average PP for the EC-free control to give a value for the peak shift. Significant peak shifts were recorded and compared to known peak positions for sucrose.

Scanning electron microscopy (SEM)

SEM was used to visualize the sucrose-EC network that was thought to be present within HRC. Samples were prepared using the SS method and included; control compound milk chocolate (Bulk Barn, Richmond Hill, ON), control with 8% EtOH, and compound milk chocolate with 2.17% EC 10 cP from a 20% solution in EtOH. The EtOH was evaporated in an incubator at 30°C for 9 days. All samples were then placed in a hexane bath for 48 h to remove all of the fat and leave behind the network of solid particles. The samples were suspended on a mesh platform about one third of the way to the top of a 400 mL glass beaker. A magnetic stir bar was placed below the mesh. The beaker was filled with approximately 300 mL of hexane and sealed with aluminum foil to prevent evaporation of the hexane. The beaker was then placed on a stir plate and set to 250 rpm. After two days of extraction the sample was removed from the beaker using tweezers and stored at room temperature in a covered dish until further use.

The samples were cut with a blade but ended up fracturing cleanly to give a good cross section of the interior of the chocolates. A small piece of the chocolate was then mounted using double sided tape onto a sample holder. The sample holder was then placed in an Emitech K550 Sputter Coater (Quorum Technologies Ltd., East Grindstead, UK) set at 20 mA for 2.5 min to give less than 20 nm of gold coating.[35] Following sputter coating samples were placed in the S-570 SEM (Hitachi High-Technologies, Tokyo, Japan). Images were obtained at various magnifications and at locations across the entire sample plane using Quartz PCI software (Quartz Imaging Corporation, Vancouver, BC) for image capture.

Interaction of EC with other particles.

The interaction between EC and various particles other than sucrose was studied to determine if sucrose is unique in its ablility to form a heat resistant network with EC. Various particles along with sucrose (superfine, Lantic Inc., Montreal, QC) were chosen to be studied based on several factors. Glucose is a monosaccharide that makes up half of the sucrose molecule and therefore it has very similar properties and structure as sucrose. Anhydrous glucose (Figure 2C) was obtained from Thermo Fisher Scientific (Ottawa, ON). Native starch is made up of amylose and amylopectin which are polymers of glucose joined by α(1-4) glycosidic bonds.[36] Amylopectin contains many branches joined by α(1-6) bonds. Native starch is also semi-crystalline. Pre-gelatinized starch has undergone a process of cooking the starch in water to dissolve the starch granule and ultimately leads to a loss of crystallinity.[36] Native and pre-gelatinized potato starch products called Novation 1900 and Novation 6600 respectively were obtained from Ingredion (Brampton, ON). Cellulose is chemically similar to starch but is a linear polymer of β(1-4) linked glucose units.[36] Microcrystalline cellulose (MCC) is a purified fraction of cellulose and as the name suggests it is highly crystalline. MCC was obtained in the form of spherical pellets called Cellets from Pharmatrans Sanaq AG (Basel, Switzerland). MCC in the form of fibers was obtained from Thermo Fisher Scientific (Ottawa, ON).

Rice bran wax (RBW) was chosen as a particle that is not similar to sucrose. Waxes are formed by the esterification of a long-chain aliphatic carboxylic acid with a long chain aliphatic alcohol.[37] They are hydrophobic and similar to the vegetable oils that are traditionally used to form organogels with EC[38] but due to their very long aliphatic chains and ester linkages they have much fewer polar functional groups. It is thought that there would be very few interactions between EC and waxes and the wax could be thought of as an inert particle. RBW was obtained from Koster Keunen, LLC (Watertown, CT). Other inert particles were also tested. Soda-lime silica glass beads were chosen as a non-crystalline inert particle and diamond dust was used as a crystalline inert particle. Glass beads were obtained from Potters Industries LLC (Valley Forge, PA) and diamond dust was obtained from Diamond Technologies Co., Ltd (Bangkok, Thailand).

Some of the materials required pre-treatments to obtain a suitable particle size. The RBW pellets were chopped using a food processor and sieved to achieve a smaller particle size. Furthermore, potato starch was chosen because the native potato starch granule is one of the largest with diameters up to 110 µm.[39, 40] However, it was not possible to obtain a commercial native potato starch that had not been milled to a fine particle size. To overcome this, finely ground native potato starch was wetted with cold water, spread onto cooking sheets and placed in the oven at 80°C. After drying the starch was broken up into small pieces and crushed in a blender for further particle size reduction. The particles were then sieved through two sieves of 70 and 170 mesh size to obtain the middle fraction with a particle size of 89-211 µm.

The sizes of all of the particles were measured using a microscopic technique. Particles were deposited on glass microscope slides and micrographs were obtained under visible light using an Olympus BX60 light microscope with an attached Olympus DP71 camera (Olympus Canada Inc., Richmond Hill, ON) used to obtain digital images. Characterization of particle size was performed using the "count/measure" function built into the ImagePro Plus 6.0 software (Media Cybernetics, Inc., Rockville, MD) which automatically determines the boundaries of each particle and then measures the mean particle diameter. A minimum of three particles were measured on each slide and seven slides were characterized for each particle type. The micrographs were also used to discuss the morphology of the particles.

Samples were prepared using the solvent substitution method explained previously. Formulas were calculated to produce samples with an equal volume fraction of each type of particle. Literature values for the density were used to calculate the mass of the particles to add to each sample to obtain the correct volume fraction. The density of RBW was easily measured using a pycnometer and a scale and this value was used for the calculations.

All of the samples were tested for hardness at 40°C using the texture analyzer method explained above. One modification to

the analysis was made; the area under the curve (AUC) from 0-3 mm compression was used as a measure of hardness instead of the force at 2 mm displacement. This was necessary because the various samples had widely different properties; for example some of the samples would fracture after 2 mm displacement. Many measures were analyzed and all showed very similar trends but the data was best represented using the AUC.

Results and discussion

Atomic scale MD simulations

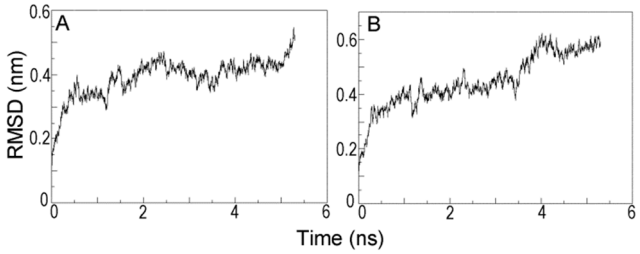

Fig. 4 RMSD of hydroxyl hydrogens on (A) ordered and (B) co-block EC polymers in triolein (simulation one)

The first set of simulation results using EC30 are described below (data not shown). These simulations predicted hydrogen bonding between the ring oxygen of EC and the hydroxyl hydrogen of sucrose. EC simulations containing multiple EC molecules have also shown the capacity for both intra- and intermolecular hydrogen bonding in which R-group hydroxyls interact with a nearby ring oxygen atom. The ability for EC to form intra- and intermolecular hydrogen bonds was expected since these interactions are necessary for EC gel formation. The formation of hydrogen bonds between hydroxylated R-groups of EC and the ether oxygen on either the sn-1 or sn-2 tails of POPC were also observed. Similarly, simulations have shown hydrogen bonds between sucrose hydroxyl groups and POPC ether groups.

A second set of simulations using ordered and co-block EC were evaluated. System one, which consisted of only EC in a sea of triolein, was analyzed for the root mean square displacement (RMSD) of the hydroxyl R-group hydrogen atoms as a function of time to examine the instability of the polar hydroxyl groups of EC in a mostly hydrophobic environment. Results showed that for both the ordered and co-block EC polymers there was an increased RMSD as a function of time (Figure 4). The RMSD corresponds to the time average of the distance between two atoms. A graph that shows a continuous increment indicates that the atoms are moving further and further apart over time. Therefore, Figure 4 indicates that the hydroxyl groups move or oscillate as they reorient themselves to minimize interactions with the hydrophobic tails of triolein by moving further away from the tails. It was also found that for the ordered and co-block polymers there were an average of 1.25 and 1.58 hydrogen bonds between the EC polymer and the ester groups on triolein respectively over the simulation time (Figures 5A and B).

In the second simulation EC was next to sucrose and surrounded by triolein. It was found that both EC polymer types were able to hydrogen bond with sucrose (Figures 5C and D). This is the same result as in the first simulation where EC was built using the shorter EC molecule. It was observed that the co-block polymer had a delay between the start of the simulation and

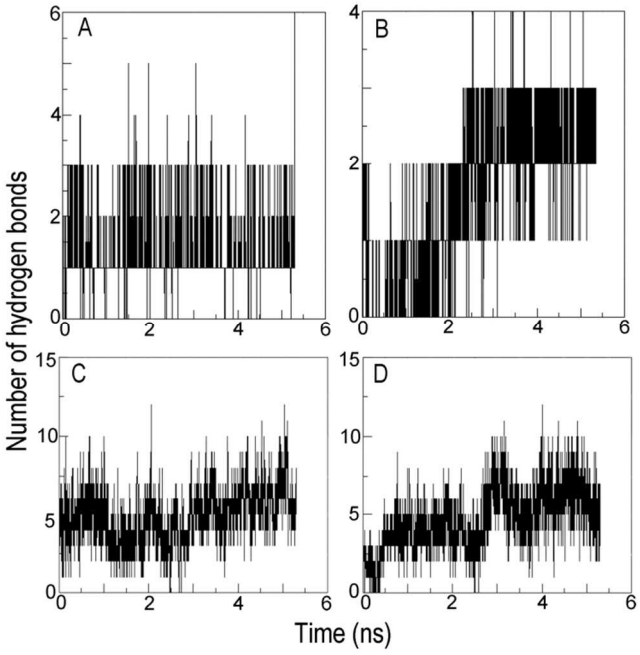

Fig. 5 Number of hydrogen bonds formed between: (A) ordered or (B) co-block EC and triolein (simulation one); and (C) ordered or (D) co-block EC and sucrose surrounded by triolein (simulation 2)

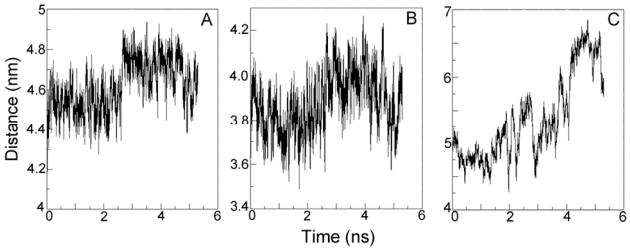

Fig. 6 Average distances between EC donor and acceptors for: (A) ordered or (B) co-block EC in simulation three; and (C) ordered EC in simulation four

reaching a relatively unchanging average number of hydrogen bonds which was not observed in the simulation with the ordered polymer. This can be attributed to twisting or shifting of the co-block polymer caused by the hydrophilic blocks of hydroxylated monomers wriggling to maximize polar contacts with sucrose and minimizing non-polar contacts. The average number of hydrogen bonds with sucrose for the ordered and co-block polymers were 4.88 and 4.66 respectively.

The third simulation had the sucrose crystals covered in POPC next to EC and surrounded by triolein. Both sucrose and EC were able to form hydrogen bonds with POPC. This mimics the result found in the first simulation with EC30. However, unlike in the first simulation, no hydrogen bonds were observed between EC and sucrose due to a shielding effect of the POPC which kept the EC at a distance too far from the sucrose for hydrogen bonds to form. The programs used to analyze the simulations require a distance between donor and acceptor of less than or equal to 0.35 nm. It was found that the average distance between EC donors and acceptors was around 4.6 and 3.9 nm for the ordered and co-block EC polymers respectively (Figures 6A and B). Again, hydrogen bonds were observed between both EC polymer types

and triolein similar to the previous simulation scenarios.

The final simulation had the EC solvated in triolein with sucrose crystals randomly placed within the simulation space. In this scenario there were no hydrogen bonds observed between either the ordered or co-block EC polymers and sucrose over the entire simulation. This was due to a large separation distance between the EC and sucrose with little attractive force to move the molecules close enough together for hydrogen bond formation (Figure 6C). The results for co-block EC were almost identical and are therefore not shown.

Overall the simulations have been successful in showing that under appropriate conditions hydrogen bonds can form between EC of various configurations and a sucrose crystal, POPC, and triolein. Further insight has also been gained into hydrogen bonding between sucrose and POPC and inter- and intra-

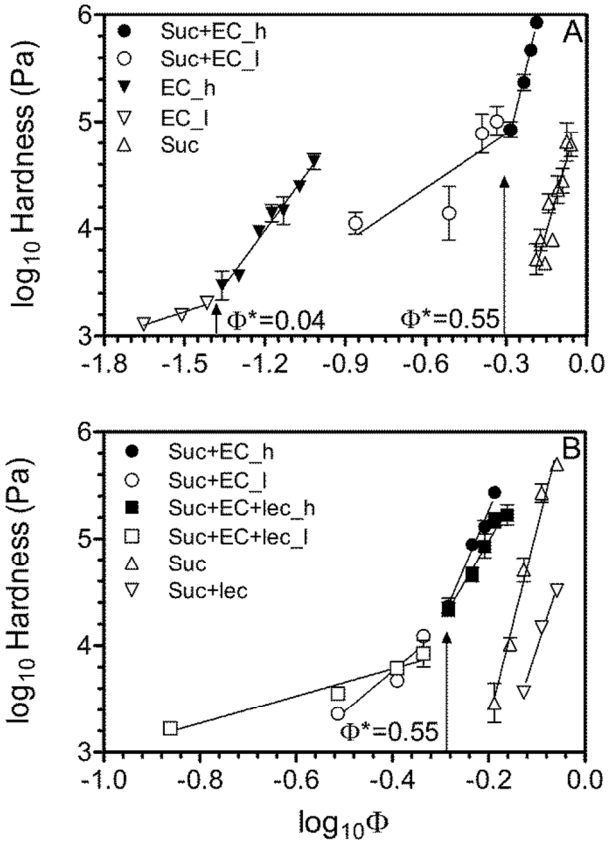

Fig. 7 Log-log plots of hardness versus volume fraction of solids (Φ) of model chocolate samples at 40°C made using the (A) solvent substitution and (B) heat methods. Suc = sucrose, lec = lecithin, h = high volume fraction samples, l = low volume fraction samples

molecular bonding of EC with EC. It has also been clearly shown that EC and sucrose surfaces must be relatively close together for hydrogen bonding to occur. Hydrogen bonding is effectively impossible between EC and sucrose when the sucrose is thoroughly surrounded by a layer of POPC. This is indicative that in a conventional chocolate if the sucrose is surrounded by POPC, other phospholipids, or perhaps any emulsifier, then the sucrose would be unable to hydrogen bond with EC and this likely negatively impacts the heat resistance of the chocolate.

Hardness tests of model systems

The hardness at increasing volume fraction of solids for samples prepared using the solvent substitution method is shown in Figure 7A. The sample with just EC and no sucrose showed low hardness values however it clearly formed a gel at volume fractions of EC around 0.04 as indicated by the discontinuity observed in the hardness values. This value was expected since previous work has shown that EC gels form at volume fractions close to 0.04[41, 42]. The sucrose control required much higher volume fractions to be solid enough for testing. These samples showed much less mechanical strength compared to the samples which contained both EC and sucrose at the same volume fractions. This indicates a synergistic effect when both EC and sucrose are present in the samples which led to very high mechanical strength. Interestingly, the samples with sucrose and EC also showed a discontinuity in values for hardness as the volume fraction (Φ) of solids increased. This behaviour is typical of a jamming transition for a granular system where a critical value Φ^* is reached when there exists just enough contacts between particles for mechanical stability to be achieved[43, 44]. Furthermore, for granular jammed systems, at $\Phi > \Phi^*$ a power law increase is expected[43, 45]. Both of these phenomena were observed in the sucrose with EC samples and indicate that below Φ^*, which was found to be 0.48-0.55, the system was in a fluid-like state and above Φ^* the system has formed a solid-like material and has great mechanical stability. These values of Φ^* match the values for a jamming transition from fluid at $\Phi < 0.494 \pm 0.002$ to solid at $\Phi > 0.545 \pm 0.002$ for a model system of hard spheres predicted by molecular dynamics simulations[44]. It is also interesting to note that the slope of the line for the sucrose with EC samples above the jamming transition was very similar to the slope for the sucrose only samples and were 10.4 ± 0.4 and 8.9 ± 0.7 respectively. This likely indicates that the two systems have very similar spatial distribution of mass and that the increased mechanical strength of the sucrose with EC system was due to enhanced interactions between the particles. Thus the EC can be thought of as glue between the sucrose particles, which is able to improve the stability and mechanical strength of the jammed solid network. Furthermore, since the sucrose-free controls showed very little mechanical strength it can be concluded that organogelation contributes minimally to heat resistance.

Similar results were observed for the samples prepared using the heat method (Figure 7B). A jamming transition was once again observed at $\Phi = 0.48$-0.55 for the sucrose with EC samples. Furthermore, the sucrose controls once again had significantly lower mechanical strength at the same Φ compared to the sucrose samples with EC. However, the sucrose control samples diplayed higher slopes indicating a slightly different spatial arrangement of mass for these samples likely due to the differences in the preparation methods, such as the slight solubility of sucrose in EtOH which will be discussed further below. This figure also shows the effect of lecithin addition. It is very obvious in the sucrose only samples that addition of lecithin reduced the mechanical strength of the samples without having a large affect on the spatial distribution of mass. This suggests the lecithin decreased the interactions between the particles but did not change how the sucrose was arranged. The same trend was observed for the samples with EC however the affect was not as dramatic. This was likely because for the samples with EC the

lecithin was not as well mixed with the sucrose since it was added with the EC and only mixed briefly. Thus, less of the lecithin would have been at the surfaces of the sucrose and would have a lesser affect on these samples. This demonstrates once again that lecithin created a boundary layer on the sucrose surface that prevented the EC from getting close enough to the sucrose to interact. This was predicted by atomic scale molecular dynamics simulations. The lecithin reduction in the hardness of the control with no EC was also expected since lecithin is known to reduce the viscosity of chocolate by aiding in the flow of fat and sucrose particles past one another.[32]

The solvent substitution and heat methods were compared and it was found that samples made via the solvent substitution method with EtOH tended to be approximately 3 times harder

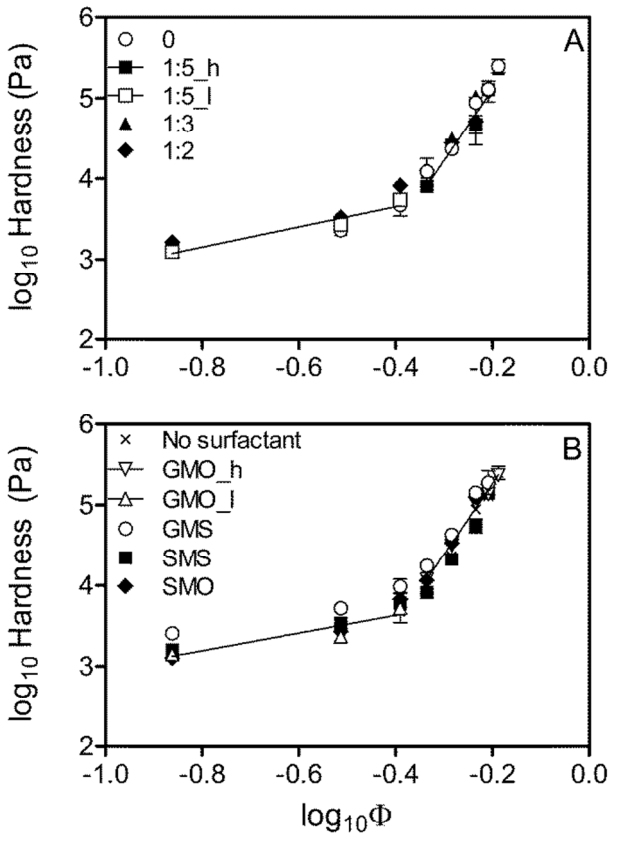

Fig. 8 Log-log plots of hardness versus volume fraction of solids (Φ) of model chocolate samples at 40°C made via the heat method with various (A) ratios of GMO:EC or (B) types of surfactant. Linear regression is shown for one sample set at h = high volume fractions and l = low volume fractions

than those made with the same amount of sucrose via the heat method. This is thought to be due to a combination of better dissolution of the EC in EtOH compared to the one in the oil phase and the slight solubility of sucrose in EtOH. Better dissolution of the EC would lead to a more extended polymer which may be better able to interact with the sucrose creating stronger inter-particle interactions. Furthermore, the solubility of sucrose in EtOH is 0.7 mg/g solution at 37°C.[46] The small portion of the sucrose that is dissolved in EtOH may enhance inter-particle interactions by causing them to stick to one another and forming recrystallized sucrose bridges between the particles once the EtOH evaporates.

Samples were prepared via the heat method with various ratios of GMO:EC to observe the impact of this surfactant on the hardness of the system. It had previously been shown that addition of surfactants to EC oleogels resulted in increases in gel strength.[47] Figure 8A shows that there were no significant differences ($P < 0.05$) in hardness for the various ratios of GMO:EC in this system. Furthermore, the jamming transition at $\Phi^* = 0.48\text{-}0.55$ followed by a power law increase in hardness was once again observed and seemed to be unaffected by increasing amounts of GMO.

Similarly, samples were prepared with various types of surfactants at a ratio of 1:3 with EC and results are shown in Figure 8B. It was found that samples made with GMS had slightly greater mechanical strength than the other samples. This was likely due to the creation of a secondary GMS network within the sample that was able to resist deformation because it was solid at 40°C. Generally, samples made with surfactant were harder than those without surfactant. The surfactant can plasticize the EC[38] allowing the polymer to be more extended in the oil which would help it to better interact with the surface of the sucrose. Generally, various surfactants produce various degrees of EC plasticization based on characteristics such as the headgroup size.[48] Though there may have been different degrees of plasticization of the EC based on surfactant ratios or types, this did not lead to any significant differences in mechanical strength of the samples. These samples also showed the jamming transition at $\Phi^* = 0.48\text{-}0.55$ followed by a power law increase in hardness. These results indicate that the strength of the EC gel had little impact on the mechanical strength observed.

Fourier transform infrared (FTIR) spectroscopy

The FTIR spectra collected had a resolution of 2 cm^{-1} and a data spacing of 1 cm^{-1}, therefore, a peak shift of 1 cm^{-1} or more is considered significant. There were very few significant peak shifts observed. However, one shift that was consistent and significant occurred at around 3335 cm^{-1}. This peak is unique to sucrose in the multi-component systems tested. Some peak shifts were also observed in the fingerprint region of the spectra for the heat samples analyzed by ATR The average change in peak position (ΔPP) for significant peak shifts are shown in Table 3.

All samples without lecithin showed the significant peak shift at 3335 cm^{-1}, although the shift was generally only one wavenumber. This peak is associated with stretching of the hydroxyl group on carbon two of the glucose ring on the sucrose molecule[34] (Figure 2A). This O(2)-H hydrogen in sucrose crystals participates in intermolecular hydrogen bonds with the oxygen on carbon 6 of the fructose moiety (O′(6)). Since the shift at 3335 cm^{-1} is to higher wavenumbers it is thought that this is indicative of weakening or loss of this intermolecular hydrogen bond when EC is present. We propose that the O(2)-H would then be available for hydrogen bonding with EC. This seems probable since the molecular simulations have shown that EC can hydrogen bond with sucrose and the hardness tests have also indicated an interaction between EC and sucrose.

The heat method samples with 2% or 5% EC also showed peak shifts to higher wavenumbers at 1346 cm^{-1} and to lower wavenumbers at 1322 and 1105 cm^{-1}. Shifts at 1346 and 1322 cm^{-1} are associated with bending of COC and COH moieties on

the sucrose respectively. The shift at 1105 cm^{-1} is attributed to stretching of a CO group. These are further indications of interactions of sucrose with EC that have lead to small changes in the molecular structure of the sucrose. These shifts were not observed in the solvent substitution samples. This may be because canola oil has peaks at similar wavenumbers and these peaks may be confounding our results.

Table 3 Peak position (PP) and average peak shifts (ΔPP) with respect to the EC-free control observed in solvent substitution and heat method samples of sucrose with EC. The values are averages of 3 replicates.

Samples	PP (cm^{-1})	ΔPP (cm^{-1})
Solvent substitution method		
16% EC on sucrose (EtOH)	3335	1
33% EC on sucrose (EtOH)	3335	1
50% EC on sucrose (EtOH)	3335	1
Heat method		
2% EC on sucrose in canola oil	3335	2
	1346	1
	1322	-1*
	1105	-1
5% EC on sucrose in canola oil	3335	1
	1346	1
	1322	-1
	1105	-2

*Negative numbers represent shifts to lower wavenumbers

Interestingly, there were no peak shifts observed in heat method samples made with lecithin coated sucrose. The presence of lecithin at the surface of sucrose prevented any bonding between sucrose and EC likely due to a shielding effect which kept the EC at too great a distance from the sucrose for interactions to occur. Again, this result confirms what was seen in the simulations and the hardness tests.

Scanning electron microscopy (SEM)

Images of the defatted chocolates (Xerogels) are shown in Figure 9. From the photographs at the top of the figure it is clear that the EC- and EtOH-containing samples held their shape throughout the defatting procedure and were able to be picked up with the tweezers with little structural damage. However, the control sample almost completely disintegrated since there was no secondary structure to hold its shape when the primary structure of solid fat was removed. Much of the solids fell through the mesh and to the bottom of the beaker. A small chunk of the control sample was left on the mesh and was able to be imaged.

It can be seen from the first row of SEM images that there are some slight differences observed between the samples. The control sample had a very smooth region with a rougher ledge to the upper right. The smooth region likely corresponds to an area where the structure has collapsed upon itself. This region would best represent the majority of the control chocolate structure considering most of the chocolate disintegrated during sample preparation. In contrast, both the EtOH control and EC sample show well defined structures with the EC sample being somewhat rougher and better defined. Perhaps this indicates that the solid particles are more tightly held together in the EC sample. Both structures have pores and crevices where the fat would be located.

The next row at a higher magnification shows slightly more detail of the above mentioned features. All samples show the smooth, straight edges of the large sucrose crystals which can be distinguished from the smaller, rough particles of cocoa powder and milk proteins. The bottom row shows a very high magnification image of the samples. Again, large sucrose particles and smaller cocoa powder and milk protein particles are visible in the control sample with a loosely piled arrangement and no apparent inter-particle structure. The EtOH control shows large sucrose crystals with other smaller particles closely packed together. There were small cocoa powder and milk protein particles and neighbouring sucrose particles stuck to all surfaces of the sucrose particles. The EC sample looked very similar to the EtOH control but displaying perhaps more aggregation. Clearly both EtOH and a combination of EC in EtOH were able to create a secondary network of solid particles within the chocolate. When the fat was removed this structure was left largely intact and would be responsible for the heat resistance in these chocolates.

Cite this: DOI: 10.1039/c0xx00000x

www.rsc.org/xxxxxx

ARTICLE TYPE

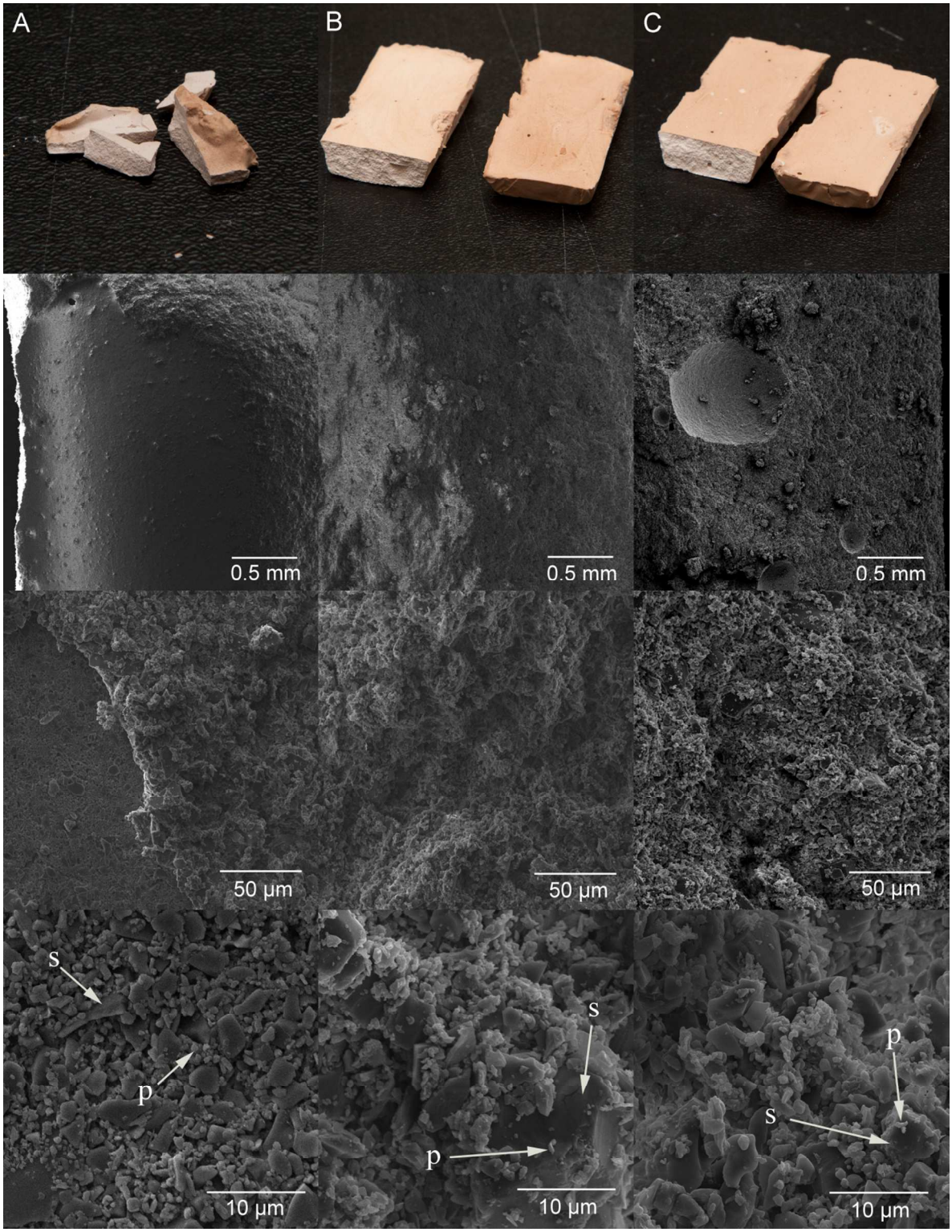

Fig.9 Photographs and SEM images of defatted chocolate samples at various magnifications. Columns show: (A) control; (B) EtOH control; and (C) 2.17% EC in chocolate. Sucrose is denoted as "s" and milk or cocoa powder is denoted by "p"

Cite this: DOI: 10.1039/c0xx00000x

www.rsc.org/xxxxxx

ARTICLE TYPE

Is the interaction of EC and sucrose particles unique?

This work has characterized in detail the interaction of EC with sucrose since this is the major component in most chocolates. This, however, does not imply that EC cannot interact with other particles in food and non-food systems. As a preliminary study in this area, we decided to use particles of similar and different chemical natures to determine if we could observe similar effects than those observed with sucrose. This could, in principle, lead to unexpected applications, or help explain certain effects. Particle size and shape was not strictly controlled in this study since the purpose of the work was to determine if particles of different chemical natures could exert the "heat resistance" effect.

Micrographs of the particles used in this study are shown in Figure 10 and show the differences in size and morphology of the particles. The average particle diameter and values for density are reported in Table 4. The particle sizes range from an average of 140-534 µm. The sucrose and glucose samples had almost identical particle sizes and were clearly individual crystals with a distinct crystalline morphology. Both starch samples, the rice bran wax (RBW) and diamond samples were more randomly shaped with rough edges. The microcrystalline cellulose (MCC) pellets and glass beads were mostly spherical in shape. Finally, the MCC fibres were not easily viewed individually due to a large amount of clumping, however there were some individual fibres viewed which are only a few micrometers thick but several tens of micrometers in length. This fibrous morphology was distinctly different from all others.

During preparation of the MCC fiber sample it was clear that there was hardly enough fat or EC in the system to sufficiently coat the surfaces of the MCC fibers. This was probably due to the fact that this sample had such a different morphology than any of the other samples. The long, thin fibers had a very large surface area compared to the other sample morphologies.

Table 4 Particle densities and average diameters with standard deviations

Particle	Density (g/mL)	Diameter (µm)
Sucrose	1.59[49]	271 ± 80
Glucose	1.54[50]	273 ± 78
Native starch	1.54[51]	193 ± 51
Pre-gelatinized starch	1.54[51]	369 ± 138
MCC pellets	1.46[52]	169 ± 40
MCC fibers	1.46[52]	140 ± 64
RBW	0.84[a]	534 ± 270
Glass beads	2.50[b]	163 ± 39
Diamond	3.52[53]	212 ± 59

[a] measured; [b] provided by the manufacturer

The results in Figure 11 show the area under the displacement in compression curve for the various treatments. This value corresponds to the energy required to compress the sample to a fixed deformation. Control samples with no EC generally required much less energy to be compressed than the samples with EC.

Cite this: DOI: 10.1039/c0xx00000x

www.rsc.org/xxxxxx

ARTICLE TYPE

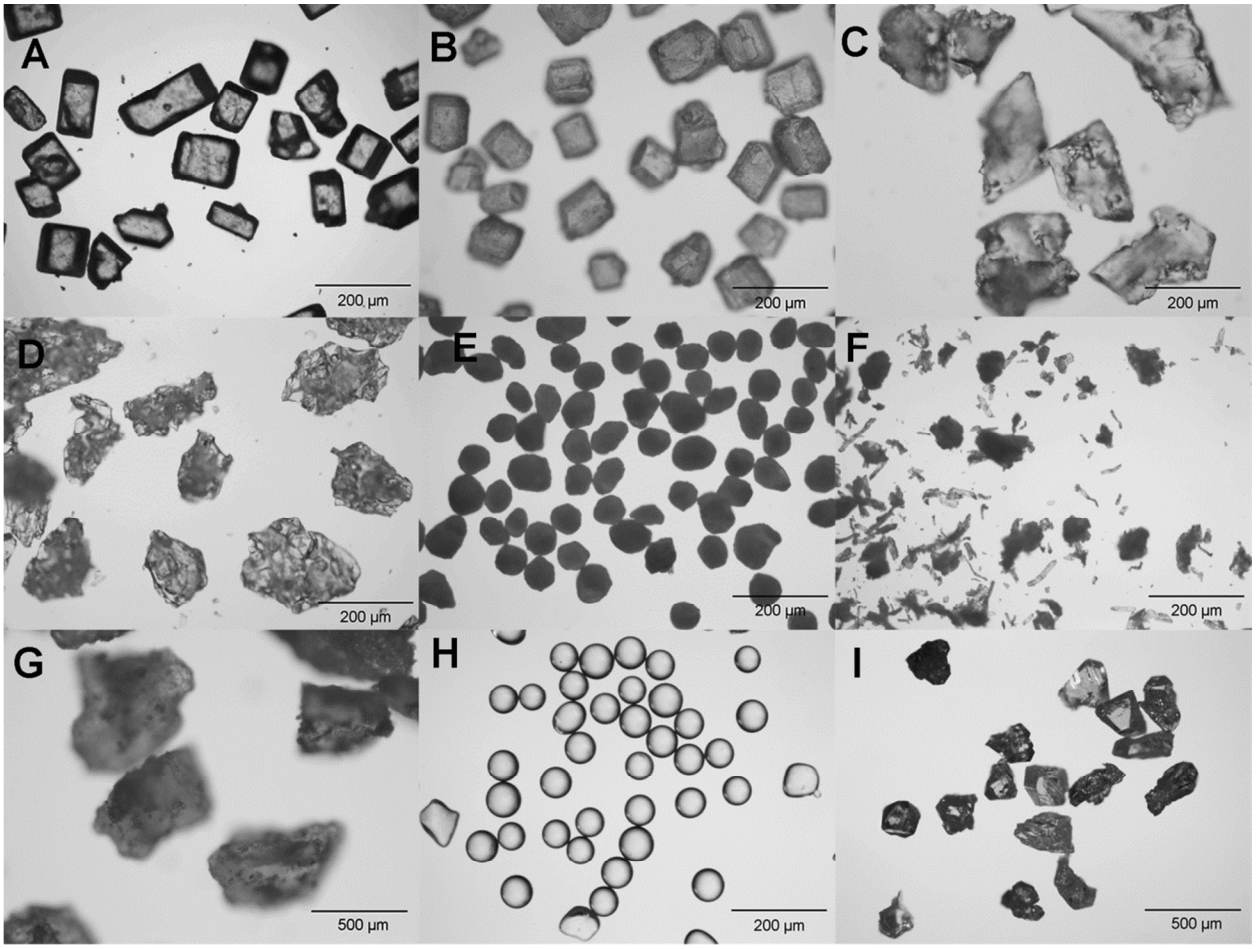

Fig.10 Micrographs of various particles: (A) sucrose; (B) glucose; (C) native starch; (D) pre-gelatinized starch; (E) MCC pellets; (F) MCC fibers; (G) RBW; (H) glass beads; and (I) diamond. Notice that RBW and diamond are shown at a higher magnification and have a scale bar measuring 500 µm while all others have a scale bar of 200 µm

Surprisingly, all of the samples tested showed some level of heat resistance upon EC addition, except for MCC fibers. Glucose, native starch, and RBW displayed an increasing energy of compression with increasing volume fraction of particles incorporated, similar to sucrose. Pre-gelatinized starch, MCC pellets, and diamond dust showed a constant energy of compression with increasing volume fraction of particles. Interestingly, the energy of compression for these samples was similar to that of the samples with the highest volume fraction of sucrose. Thus, similar heat resistance could be achieved with particles other than sucrose. This,does not imply that chocolate should be made with diamonds, but rather than several different particles can interact with EC, enhance the mechanical strength of networks formed with these particles and thus exert secondary effects, such as heat resistance. Future work should include studies focusing on EC-particle interactions where network strength enhancement is sought. The exact nature of the EC-particle interactions for some of these other particles, such as diamond, glass and rice bran wax, were not determined.

Cite this: DOI: 10.1039/c0xx00000x

www.rsc.org/xxxxxx

ARTICLE TYPE

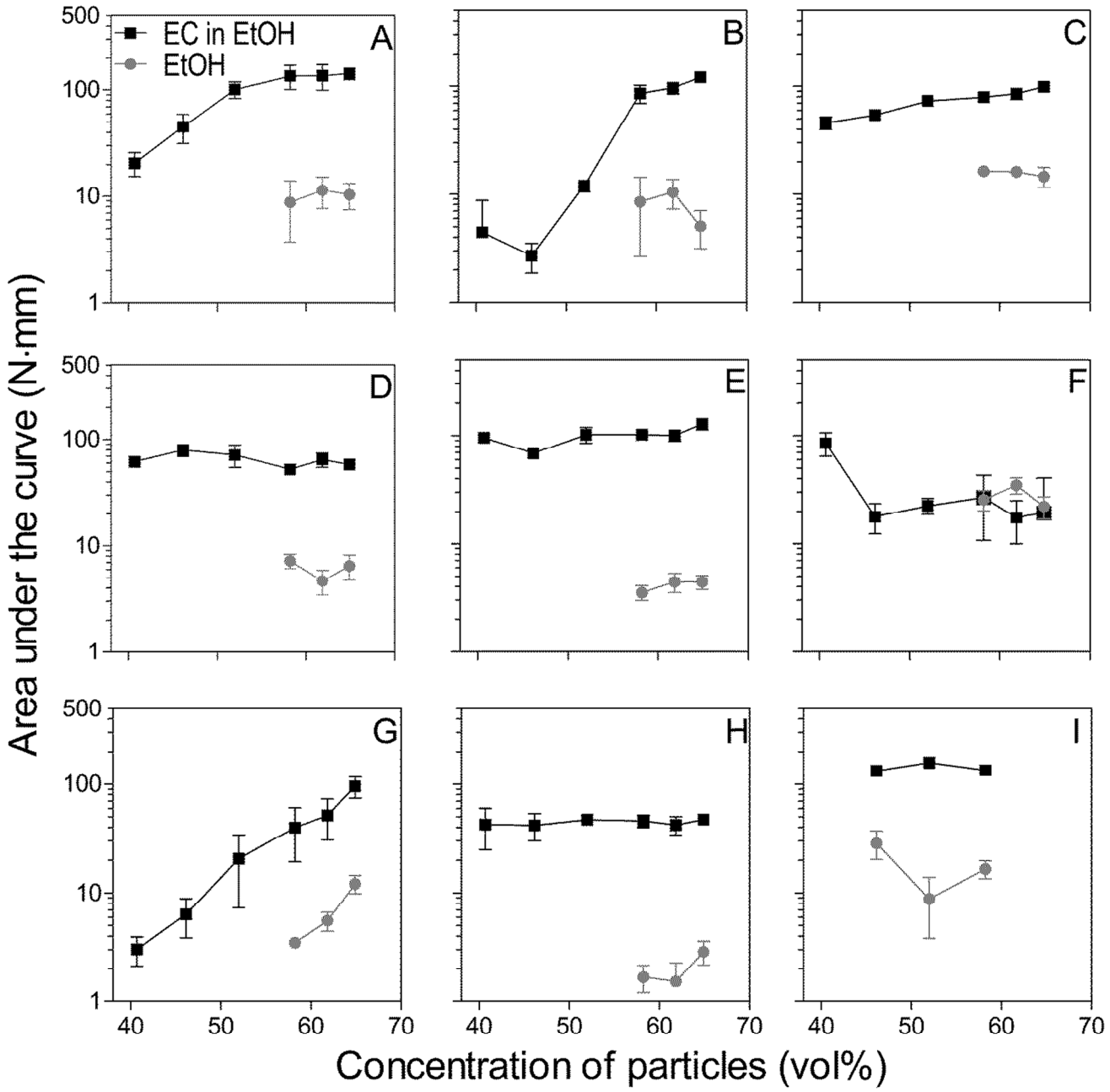

Fig.11 Area under the displacement in compression curve at 40°C for samples made with various particles at increasing particle concentration and constant EC concentration. (A) sucrose; (B) glucose; (C) native starch; (D) pre-gelatinized starch; (E) MCC pellets; (F) MCC fibers; (G) RBW; (H) glass beads; (I) diamond. Values represent the average and standard deviation. Black squares are the particles treated with EC in EtOH and grey circles are the control particles treated with only EtOH

Conclusions

In this study, we show by multiple methods that EC and sucrose can interact. MD simulations and FTIR have indicated that these interactions are due to hydrogen bonding between polar groups on the EC and sucrose. These interactions lead to structure formation within chocolate samples and this structure was responsible for heat resistance. It was also found that when lecithin was added to the system as a coating on the sucrose

crystals hydrogen bonding between EC and sucrose was hindered. This resulted in a sample with reduced heat resistance due to the lack of a sucrose-EC network. Finally, the interactions between EC and sucrose were not unique; network formation also occurred with other particles including glucose, starch, wax, glass and diamond.

References

Depts. of [a]Food Science and [b]Biophysics Interdepartmental Group (BIG), University of Guelph, 50 Stone Road East, Guelph, ON, N1G 2W1 Canada; Fax: +1 519 824 6631; Tel: +1 519 824 4120 x5434 E-mails: tstortz@uoguelph.ca; demourad@uoguelph.ca; amarango@uoguelph.ca [c]Departments of Sustainability Science and Chemistry, Lakehead University, Orillia,ON, L3V 0B9 Canada; E-mail: tlaredo1@lakeheadu.ca

1 T. A. Stortz and A. G. Marangoni, *Food Res. Int.,* 2013, **51**, 797-803.
2 J. M. DeMan, *Principles of food chemistry*, Aspen Publishers, Inc., Gaithersburg, Maryland, 1999.
3 T. A. Stortz and A. G. Marangoni, *Trends Food Sci. Technol.,* 2011, **22**, 201--214.
4 *US Pat.,* 2904438, 1959.
5 *US Pat.,* 2487931, 1949.
6 *US Pat.,* 2760867, 1956.
7 K. Rosell, *Carbohydr. Res.,* 1988, **177**, 289-298.
8 S. P. Rowland, E. J. Roberts and J. L. Bose, *J. Polym. Sci. A-1 Polym. Chem.,* 1971, **9**, 1431-1440.
9 J. Reuben, *Carbohydr. Res.,* 1987, **161**, 23-30.
10 J. S. Mahoney and C. B. Purves, *J. Am. Chem. Soc.,* 1942, **64**, 15.
11 H. Ibrahim, E. Sallam, M. Takieddin and M. A. Shamat, *Drug Dev. Ind. Pharm.,* 1988, **14**, 1249-1276.
12 S. C. Porter, *Drug Dev. Ind. Pharm.,* 1989, **15**, 1495-1521.
13 E. Lizaso, M. E. Muñoz and A. Santamaría, *Macromolecules,* 1999, **32**, 1883-1889.
14 P. W. S. Heng, L. W. Chan and K. T. Chow, *Pharm. Res.,* 2005, **22**, 676-684.
15 J. Huang, R. J. Wigent and J. B. Schwartz, *J. Pharm. Sci.,* 2008, **97**, 251-262.
16 T. Laredo, S. Barbut and A. G. Marangoni, *Soft Matter,* 2011, **7**, 2734-2743.
17 A. J. D'Ambra, M. J. Rice, S. G. Zeller, P. R. Gruber and G. R. Gray, *Carbohydr. Res.,* 1988, **177**, 111-116.
18 B. Hess, C. Kutzner, D. van der Spoel and E. Lindahl, *J. Chem. Theory Comput.,* 2008, **4**, 435-447.
19 D. van der Spoel, E. Lindahl, B. Hess, G. Groenhof, A. E. Mark and H. J. C. Berendsen, *J. Comput. Chem.,* 2005, **26**, 1701-1718.
20 E. Lindahl, B. Hess and D. van der Spoel, *J. Mol. Model.,* 2001, **7**, 306-317.
21 H. J. C. Berendsen, D. van der Spoel and R. van Drunen, *Comput. Phys. Commun.,* 1995, **91**, 43-56.
22 D. van der Spoel, A. R. van Buuren, Apol,E.,Meulenhoff,P.J., D. P. Tieleman, A. L. T. M. Sijbers, B. Hess, K. A. Feenstra, E. Lindahl, R. van Drunen and H. J. C. Berendsen, *Gromacs user manual version 3.1.1*, Groningen, The Netherlands. Internet: www.gromacs.org, 2002.
23 C. Oostenbrink, A. Villa, A. E. Mark and W. F. Van Gunsteren, *J. Comput. Chem.,* 2004, **25**, 1656-1676.
24 R. D. Lins and P. H. Hünenberger, *J. Comput. Chem.,* 2005, **26**, 1400-1412.
25 H. S. Hansen and P. H. Hünenberger, *J. Comput. Chem.,* 2011, **32**, 998-1032.
26 A. K. Malde, L. Zuo, M. Breeze, M. Stroet, D. Poger, P. C. Nair, C. Oostenbrink and A. E. Mark, *J. Chem. Theory Comput.,* 2011, **7**, 4026-4037.
27 D. P. Tieleman and H. J. C. Berendsen, *Biophys. J.,* 1998, **74**, 2786-2801.
28 H. J. C. Berendsen, J. P. M. Postma, W. F. van Gunsteren, A. DiNola and J. R. Haak, *J. Chem. Phys.,* 1984, **81**, 3684-3690.
29 G. Bussi, D. Donadio and M. Parrinello, *J. Chem. Phys.,* 2007, **126**.
30 M. Parrinello and A. Rahman, *J. Appl. Phys.,* 1981, **52**, 7182-7190.
31 Avogadro: an open-source molecular builder and visualization tool (Version 1.0.3), 2011, available from http://avogadro.openmolecules.net/.
32 S. T. Beckett, *The science of chocolate*, The Royal Society of Chemistry, Cambridge, UK, 2000.
33 F. D. Gunstone and J. L. Harwood, in *The lipid handbook,* ed. F. D. Gunstone, J. L. Harwood and A. J. Dijkstra, CRC Press, Boca Raton, FL, 2012, pp.37-91.
34 H. A. Tajmir-Riahi, *J. Inorg. Biochem.,* 1987, **31**, 255-265.
35 Quorum Technologies Ltd., *K550X Sputter coater instruction manual,* 2007, http://www.quorumtech.com/pdf/currentProductInstructionManuals/K550X_Instruction_Manual.pdf, (accessed October 3 2013).
36 J. N. BeMiller and K. C. Huber, in *Fennema's food chemistry,* ed. S. Damodaran, K. L. Parkin and O. R. Fennema, CRC Press, Boca Raton, FL, 2008, pp.83-154.
37 D. J. McClements and E. A. Decker, in *Fennema's food chemistry,* ed. S. Damodaran, K. L. Parkin and O. R. Fennema, CRC Press, Boca Raton, FL, 2008, pp.155-216.
38 T. Dey, D. A. Kim and A. G. Marangoni, in *Edible Oleogels: Structure and Health Implications,* ed. A. G. Marangoni and N. Garti, AOCS Press, Urbana, Illinois, 2011, pp.295-311.
39 N. Singh and L. Kaur, *J. Sci. Food Agric.,* 2004, **84**, 1241-1252.
40 J. Jane and J. J. Shen, *Carbohydr. Res.,* 1993, **247**, 279-290.
41 J. M. Aiache, P. Gauthier and S. Aiache, *Int. J. Cosmetic Sci.,* 1992, **14**, 228-234.
42 P. Gauthier, S. Aiache and J. M. Aiache, *Int. J. Cosmetic Sci.,* 1996, **18**, 229-235.
43 T. S. Majmudar, M. Sperl, S. Luding and R. P. Behringer, *Phys. Rev. Lett.,* 2007, **98**, 058001.
44 C. P. Goodrich and A. J. Liu, *Phys. Rev. Lett.,* 2012, **109**, 095704.
45 C. Radin, *J. Stat. Phys.,* 2008, **131**, 567-573.
46 A. Bouchard, G. W. Hofl and G. Witkamp, *J. Chem. Eng. Data,* 2007, **52**, 1838-1842.
47 A. J. Gravelle, S. Barbut and A. G. Marangoni, *Food Funct.,* 2013, **4**, 153.
48 E. D. Co and A. G. Marangoni, *J. Am. Oil Chem. Soc.,* 2012, **89**, 749-780.
49 J. Elversson and A. Millqvist-Fureby, *J. Pharm. Sci.,* 2005, **94**, 2049-2060.
50 B. A. Malik and M. Benaissa, in *Dietary sugars: chemistry, analysis, function and effects,* ed. V. R. Preedy, The Royal Society of Chemistry, Cambridge, UK, 2012, pp.79-85.
51 A. W. Newman, R. I. Mueller, I. M. Vitez, C. C. Kiesnowski, D. E. Bugay, W. P. Findlay and C. Rodriguez, in *Analytical profiles of drug substances and excipients,* ed. H. G. Brittain, Academic Press, Inc., San Diego, California, 1996, pp.523-578.
52 C. C. Sun, *J. Pharm. Sci.,* 2005, **94**, 2132-2134.
53 Y. Lifshitz, G. D. Lempert, S. Rotter, I. Avigal, C. Uzan-Saguy, R. Kalish, J. Kulik, D. Marton and J. W. Rabalais, *Diam. Relat. Mater.,* 1994, **3**, 542-546.

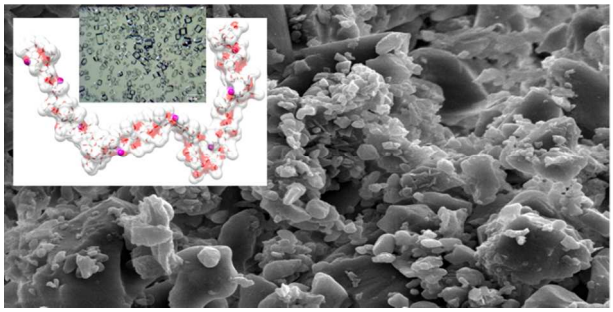

Heat resistance in chocolate upon ethylcellulose addition is due to the formation of a jammed sugar network